Modeling the clearance of hyaluronan: an approach to estimating lymph flow

Martin Fink, Andreas Rössler and Jerry J Batzel

April, 2004

Abstract

One of the important factors in blood pressure regulation is the maintenance of the blood volume, which depends on several factors including the role of lymphatics. To get an estimation of the fluid volume distribution and the overall dynamics, it would be necessary to know lymph flow dynamics. This model is an approach to assess the lymph flow by measurements of the substance hyaluronan (HA), which is transported by the lymph flow from the interstitium to the plasma. A six compartment model is presented in this paper, which is able to emulate the steady state relationships and qualitatively the dynamics.

Sensitivity analysis shows that during ultrafiltration the lymph flow is one of the main parameters which influence the total HA level. This suggests that the model may produce good results in estimating the lymph flow.

Further investigations and parameter estimation will be done with data showing the dynamics of small and large HA molecules.

Contents

1 Hyaluronan (HA)

1.1 Some facts about HA

HA, discovered by Meyer and Palmer in 1934, is an unbranched linear polysaccharide chain of alternating units of glucuronic acid and N-acetylglucosamine that is linked glycosidically via the 1-4 positions of the sugar rings [1, 2]. HA is built by fibroblasts and a major constituent of the extracellular matrix and lymph fluid [3]. Through its contribution to osmotic pressure and resistance to flow, it takes part in the regulation of tissue hydration and is an important determinant for hydraulic conductivity and macromolecular transport properties of the interstitium [4]. Biological roles of HA include stabilization of the loose connective tissue, maintenance of water and protein homeostasis, protection of cells from potentially harmful effects of other cells and microorganisms, and modulation of the inflammatory reaction [5]. Variation in the content and concentration of HA may therefore affect interstitial fluid characteristics like hydrostatic pressure and volume. The interstitial fluid hydraulic pressure is in turn an important determinant of the rate of change of plasma volume. The compliance of the interstitial fluid compartment is very high, so that the interstitial fluid hydraulic pressure remains low over a wide range of expanded interstitial volumes and becomes in fact strongly negative as the interstitial volume falls below normal [6]. The result of this is a decrease in water transfer to the vascular compartment as the interstitial hydraulic pressure is reduced and becomes negative.

1.2 Kinetics of HA fragments

Another important point about the characteristics of HA is that this molecule is characterized by an extremely high turn over (halftime of 0.5 day in skin and joints indicating that about a third of HA in the human body is removed and replaced each day), resulting in the generation of fragments from larger precursor molecules. In contrast to protein bound immobilized glycosaminoglycans, HA is able to enter the lymphatics. Here its concentration (0.2–50 mg/L) is 10 to 100 times higher than in plasma [7], suggesting that the lymphatic route may be a major supply of HA in plasma.

Intriguingly, most degradation (ca. 90 %) occurs not locally in the tissues, but within distant lymph nodes that are not only capable to catabolize, but even to produce low (< 10 kD) and high (range of 140 kD) molecular fragments of HA (LMWHA & HMWHA respectively) and to release them into the bloodstream [8, 9], where they act physiologically in an antagonistic fashion [10]. The degradation (shredding) of the hyaluronan molecules into the two weight groups within the lymph nodes depends on the time the molecules need to reach the plasma, where there is no shredding and thus the molecules are preserved unchanged until they are excreted. The time that HA remains in the lymph nodes depends on the rate of the overall lymph flow.

HA fragments within the bloodstream

When HA reaches the blood, it is mainly cleared by the hepato-splanchnic region which plays a major role in the biodegradation of endogenous circulating HMWHA. About 25 % of the plasma HA content is eliminated every minute. Thus, an increased portal blood pressure for instance in liver cirrhosis and therefore increased lymph flow from the splanchnic region might be responsible for elevated serum HA levels in these patients.

Once within the bloodstream, HMWHA cannot pass the glomerular barrier due to its molecular weight of 50–250 kDa and is therefore exclusively cleared by the liver. Elimination of HMWHA happens by a molecular weight dependent receptor uptake [11]. The higher affinity of the liver endothelial cells for the HMWHA species will leave LMWHA circulating for a longer time, as they have to be cleared by the kidneys [7].

It must be mentioned that the avidity of binding of LMWHA to the receptors in the liver increases with oligomeric size up to 38 sugars and binding of HMWHA is inhibited by HA-derived oligosaccharides of between six and 18 sugars [12]. While both types of HA fragments bind to specialized liver cells, only the large ones are eliminated by the liver and this uptake is competitively inhibited by the occurrence of LMWHA. Another important difference between the kinetics of these two molecular groups is their passage across the vascular wall. LMWHA has the ability to tunnel through capillary walls, which is impossible for HMWHA [7, 13].

Resulting from these different kinetics, a normal total HA concentration in plasma is between 30 and 40 μg/L, but it may vary from 10 to 100 μg/L and more than 80 % of total HA represents HMWHA. Hence, circulating level of HA reflects the dynamic state between delivery to and removal from the bloodstream, whereas the plasma half-life of this molecule once entered into the bloodstream is 3 to 5 minutes [14]. Moreover, external factors like diet, circadian rhythms, orthostatic stress and some clinical disorders were shown to influence the level of plasma HA to a different degree [15].

1.3 Lymphatics

Though 60–70 % of the body mass is water, only a small part of this volume is located in the blood circulation and about 12 L is stored within the interstitial space. Only about 3 L of water and a large amount of red blood cells make up the 5 L of blood circulating in the blood vessels. Several factors, such as drinking, renal excretion, ultrafiltration at dialysis, and also orthostatic stress change the amount of plasma volume. The fluid balance between interstitium and plasma is maintained by two mechanisms: the lymph flow and the microvascular filtration, but the role of the lymphatics during orthostasis in largely unknown.

The lymph flow is a slow flow from the interstitium to the plasma at about 2 mL/min, which can be controlled by adapting the lymphatics (small lymph vessels).

Starling found that microvascular filtration $Q_{\mathrm{f,PI}}$, i.e., the exchange of water between capillaries and interstitium, can be determined by the net effect of four pressures

$$Q_{\mathrm{f,PI}} = K_{\mathrm{f}}(p_{\mathrm{C}} - p_{\mathrm{I}} - \pi_{\mathrm{P}} + \pi_{\mathrm{I}}),$$

where K_{f} is the capillary filtration coefficient which reflects the membrane conductivity, p_{C} is the capillary pressure, p_{I} the interstitial pressure, and π_{P} and π_{I} are the colloid osmotic pressures for plasma and interstitium, respectively.

This represents a passive effect which depends on the pressures (and thus on the volumes) and on the protein concentrations of the interstitium and the plasma.

Orthostatic stress and the lymphatics

During orthostasis the blood capillary pressure in the lower extremities is high, promoting fluid filtration into the interstitium. Several factors operate to limit this filtration [16]; the quantitative contribution of the lymphatic system during standing is unknown, the resting supine limb lymph flow may even be nil [17].

In the sitting position, however, interstitial fluid is drained by the lymphatics, most probably a result of intrinsic contractions, which actively propel lymph fluid [18].

A high flow of concentrated lymph is observed during the first hour of standing position, conceivably because venous expansion pushes interstitial fluid into the lymphatic system. Furthermore the lymph becomes diluted due to the addition of water coming from the vascular compartment.

A delayed and gradual increase of lymph flow seems to be a response to orthostasis and local peripheral stasis [19].

Reduction of lymph flow during venous stasis has also been reported, possibly due to tonic contraction and reduced lymph propulsion mediated by lymphatic nerves or by overflow of norepinephrine from adjacent vessels [20].

Even lymphatic sequestration may also occur during the changes in transmural pressure that are associated with orthostatic stress. Increase of interstitial fluid volume together with passive dilation of the lymphatics during orthostasis would promote the movement of fluid volume from the interstitium into lymphatic capillaries [21], but recovery of fluid volume from the lower body may be delayed due to a slow reflux of thoracic duct lymph to the bloodstream.

Lymph flow in the leg is low during rest in a horizontal position, on average 0.24 mL/h, but increases 10 times during activities in the erect position [22].

Orthostatic stress alters the distribution of Starling forces within the capillaries in the different parts of the body, together with lymphatic return. Consequently the filtration balance is disturbed and fluid shifts occur immediately which influence blood and plasma volume, plasma protein concentration, oncotic pressure, hematocrit, hemoglobin concentration, local tissue hydration, and also total body water [23].

To get estimation on the fluid volume distribution and the overall dynamics, it would be necessary to know the lymph flow dynamics.

1.4 Orthostasis and HA

With orthostasis, the distribution of blood to the organs and tissues changes markedly; blood flow to the viscera and liver falls and flow to the periphery increases. Thus a change in posture should contribute to changed plasma HA level. Assuming a plasma flow of 800 and 600 mL/min [24] in normal liver and kidneys, respectively, the average normal plasma clearances of HA in these organs in the resting subject may be estimated to be 250 and 120 mL/min, respectively [25].

An increased interstitial hydration and increased lymph flow may facilitate removal of HA from the interstitial space. Slight body tilting or assumption of the upright position after prolonged rest is followed by a 3–5-fold rise in the mean lymph flow. This effect lasts for about 1 hour, and then a slight decrease can be observed [26]. Consequently a high flow of HA concentrated lymph should be observed during the first hour of standing position, as venous expansion pushes interstitial fluid into the lymphatic system. A delayed and gradual increase of lymph flow seems to be a response to orthostasis [19] and local peripheral stasis [27]. Thus an increased lymph flow into the venous system by the way of the thoracic duct should be visible in elevated HA concentrations in plasma.

1.5 Goal of the model

A key element to understanding the overall fluid exchange dynamics is the lymphatic flow. Knowledge of this flow is an important quantity in maintaining the blood volume in cases when fluid shifts occur, such as haemodialysis and/or orthostasis. Our proposed model is an approach to estimate the lymph flow by measurements of the two fragments of HA, which is transported via the lymph flow from the interstitial space to the plasma. Taking into account the different kinetics and properties of these fragments, we propose a model, which is able to estimate fluid shifts from the interstitial space via the lymphatics to the plasma during different conditions, such as orthostasis or haemodialysis.

2 Model

2.1 ODE system

The model we developed to describe the hyaluronan dynamics consists of a system of six ordinary differential equations describing mass balance relations, where Equations (2.1–2.4) consider the dynamics of HA and Equations (2.5–2.6) reflect the fluid distribution changes:

$$\frac{d}{dt}m_{\mathrm{m,P}} = J_{\mathrm{m,LP}} - J_{\mathrm{m,PHep}}, \tag{2.1}$$

$$\frac{d}{dt}m_{\mathrm{o,P}} = J_{\mathrm{o,LP}} - J_{\mathrm{o,PI}} - J_{\mathrm{o,PRen}} - J_{\mathrm{o,PDia}}, \tag{2.2}$$

$$\frac{d}{dt}m_{\mathrm{m,L}} = J_{\mathrm{m,0L}} - J_{\mathrm{m,LP}} - J_{\mathrm{mo,L}}, \tag{2.3}$$

$$\frac{d}{dt}m_{\mathrm{o,L}} = J_{\mathrm{mo,L}} + J_{\mathrm{o,PI}} - J_{\mathrm{o,LP}}, \tag{2.4}$$

$$\frac{d}{dt}V_{\mathrm{P}} = Q_{\mathrm{LP}} - Q_{\mathrm{f,PI}} - Q_{\mathrm{uf,P}}, \tag{2.5}$$

$$\frac{d}{dt}V_{\mathrm{I}} = Q_{\mathrm{f,PI}} - Q_{\mathrm{LP}}, \tag{2.6}$$

where subscript 'm' denotes macromolecular hyaluronan (HMWHA) and subscript 'o' oligomeric hyaluronan (LMWHA), 'P' refers to plasma values, 'I' to interstitial, and 'L' to lymph variables (though most often we equate the lymph with the interstitium), and '0' indicates constant production over time.

Thus, $m_{\mathrm{m,P}}$ and $m_{\mathrm{o,P}}$ are the masses of HMWHA and LMWHA in the blood plasma and $m_{\mathrm{m,L}}$ and $m_{\mathrm{o,L}}$ are the respective concentrations in the lymph, whereas V_{P} is the fluid volume in the plasma and V_{I} the interstitial fluid volume.

The flows

$J_{\mathrm{m,LP}}$ and $J_{\mathrm{o,LP}}$ denote the respective molecule flow from the lymph system into the plasma and $J_{\mathrm{m,0L}}$ represents the inflow of HMWHA into the lymph (coming from "external" production sites) and $J_{\mathrm{mo,L}}$ the degradation from macro to oligomeric molecules in the lymph. $J_{\mathrm{o,PI}}$ represents the reverse flow of LMWHA from the plasma into the interstitial space at the capillaries.

$J_{\mathrm{m,PHep}}$, $J_{\mathrm{o,PRen}}$ and $J_{\mathrm{o,PDia}}$ denote the excretion of the respective molecules by liver, kidney, and dialysis.

Q_{LP} denotes the lymph flow, $Q_{\mathrm{f,PI}}$ the microvascular filtration (fluid exchange between plasma and interstitium), and $Q_{\mathrm{uf,P}}$ the amount of ultrafiltration from the plasma in dialysis.

We will first describe the auxiliary equations for the hyaluronan modeling part and afterwards the auxiliary equations for the fluid volumes. See Tables 1 and 2 for parameter values.

2.2 Hyaluronan auxiliary equations

Production and degradation of hyaluronan

The production process of hyaluronan is very complicated and too many details are unknown or remain to be clarified. Very large hyaluronan molecules are transported to the lymph and there degraded into HMWHA and LMWHA.

We assume for this preliminary model that the production rate is constant and thus there is a constant inflow of macromolecular HA into the lymph:

$$J_{\mathrm{m,0L}} = K_{\mathrm{m,0L}}, \tag{2.7}$$

where $K_{\mathrm{m,0L}}$ is different for healthy individuals and dialysis patients.

The degradation of unshredded as well as macromolecular HA is dependent on the resting time of the molecules in the lymphatic nodes, which is dependent on the lymph flow Q_{LP} and is summarized in one process:

$$J_{\mathrm{mo,L}} = c_{\mathrm{m,L}} e^{-K_{\mathrm{mo,L}} Q_{\mathrm{LP}}}, \tag{2.8}$$

where $c_{\mathrm{m,L}}$ is the concentration of macromolecular HA in the lymph and $K_{\mathrm{mo,L}}$ the speed of degradation.

Hyaluronan flows from the lymph into the plasma

Hyaluronan is expelled from lymph by the flow into the plasma. When it reaches the plasma the degradation process stops and no further conversion occurs.

The molecule flows of macromolecular $J_{\mathrm{m,LP}}$ and oligomeric $J_{\mathrm{o,LP}}$ hyaluronan entering the plasma by the lymph flow are described by

$$J_{\mathrm{m,LP}} = c_{\mathrm{m,L}} Q_{\mathrm{LP}}, \tag{2.9}$$
$$J_{\mathrm{o,LP}} = c_{\mathrm{o,L}} Q_{\mathrm{LP}}, \tag{2.10}$$

where Q_{LP} is the actual lymph flow and $c_{\mathrm{m,L}}$ and $c_{\mathrm{o,L}}$ represent the concentration of hyaluronan in the lymph nodes.

Diffusion of small molecules through the vessel walls

The small molecules are not only transported by the lymph flow, but can also filtrate back from the plasma into the interstitium through the capillary vessel walls. A possible approach to model this exchange is

$$J_{\mathrm{o,PI}} = K_{\mathrm{o,PI}} c_{\mathrm{o,P}}, \tag{2.11}$$

where $K_{\mathrm{o,PI}}$ is the fraction of LMWHA in the plasma which is tunneling through the capillary walls per minute.

Enzyme kinetics in the kidney

The enzyme kinetics for clearance in the kidney are described using the approximation given by the Michaelis–Menten excretion rate. In this process the enzyme E converts substrate S into the product P by first combining with S to form complex C and then breaking down into P and E:

$$\mathrm{S} + \mathrm{E} \underset{\mathrm{k}_{-1}}{\overset{\mathrm{k}_1}{\rightleftarrows}} \mathrm{C} \xrightarrow{\mathrm{k}_2} \mathrm{P} + \mathrm{E}. \tag{2.12}$$

The quasi-steady-state and the equilibrium approximation of these dynamics determine a reaction velocity v given by

$$v = \frac{\bar{v} s}{K_s + s}, \tag{2.13}$$

with $\bar{v}$ the maximal reaction velocity, s concentration of the substrate S and K_s the Michaelis–Menten constant (see [28]).

Denoting the renal compartment with subscript "ren", the excretion rate from the kidneys of the small hyaluronan molecules is given by

$$\tilde{J}_{\mathrm{ren}} = \frac{\bar{v}_{\mathrm{o,Ren}} c_{\mathrm{o,P}}}{K_{\mathrm{o,Ren}} + c_{\mathrm{o,P}}}, \quad \text{with } c_{\mathrm{o,P}} = \frac{m_{\mathrm{o,P}}}{V_{\mathrm{P}}}, \tag{2.14}$$

where $c_{\mathrm{o,P}}$ is the plasma concentration of oligomeric hyaluronan molecules and V_{P} denotes the blood plasma volume. Macromolecules are not excreted through the kidney.

Competitive binding at the liver

The clearance kinetics of the larger hyaluronan molecules in the liver can be described in a similar way. The difference is that not only the large molecules bind to the liver, but also the small molecules bind, but without being excreted. Thus the small molecules act to inhibit large molecule excretion.

Adding a competitive inhibitor to the kinetics of (2.12) we get (see [28])

$$\mathrm{S} + \mathrm{E} \underset{\mathrm{k}_{-1}}{\overset{\mathrm{k}_1}{\rightleftarrows}} \mathrm{C} \xrightarrow{\mathrm{k}_2} \mathrm{P} + \mathrm{E}, \tag{2.15}$$

$$\mathrm{I} + \mathrm{E} \underset{\mathrm{k}_{-3}}{\overset{\mathrm{k}_3}{\rightleftarrows}} \mathrm{C}_2, \tag{2.16}$$

where I denotes the inhibitor (in our case the small molecules) which inhibit the binding of the big molecules to the liver. The reaction velocity in this case is given by

$$v = \frac{\bar{v}s}{K_s + s\left(1 + \frac{i}{K_i}\right)}, \tag{2.17}$$

where i is the concentration of the inhibitor and $K_i = k_{-3}/k_3$.

For our model this becomes

$$\tilde{J}_{\mathrm{hep}} = \frac{\bar{v}_{\mathrm{m,Hep}} c_{\mathrm{m,P}}}{K_{\mathrm{m,Hep}} + c_{\mathrm{m,P}}\left(1 + \frac{c_{\mathrm{o,P}}}{K_{\mathrm{o,Hep}}}\right)}, \quad \text{with } c_{\mathrm{m,P}} = \frac{m_{\mathrm{m,P}}}{V_{\mathrm{P}}}, \tag{2.18}$$

where $c_{\mathrm{m,P}}$ and $c_{\mathrm{o,P}}$ are the plasma concentrations of the larger resp. smaller hyaluronan molecules and "hep" denotes the liver compartment.

Dependency on blood flow to liver and kidney

The amounts of excretion $J_{\mathrm{o,PRen}}$ and $J_{\mathrm{m,PHep}}$ depend also on the blood flow to the organs, thus we get the relations

$$J_{\mathrm{o,PRen}} = Q_{\mathrm{Ren}} \tilde{J}_{\mathrm{ren}} = \frac{Q_{\mathrm{Ren}} \bar{v}_{\mathrm{o,Ren}} c_{\mathrm{o,P}}}{K_{\mathrm{o,Ren}} + c_{\mathrm{o,P}}}, \tag{2.19}$$

$$J_{\mathrm{m,PHep}} = Q_{\mathrm{Hep}} \tilde{J}_{\mathrm{hep}} = \frac{Q_{\mathrm{Hep}} \bar{v}_{\mathrm{m,Hep}} c_{\mathrm{m,P}}}{K_{\mathrm{m,Hep}} + c_{\mathrm{m,P}}\left(1 + \frac{c_{\mathrm{o,P}}}{K_{\mathrm{o,Hep}}}\right)}. \tag{2.20}$$

Dialysis filter

The dialysis filter at ultrafiltration is assumed to filter a constant proportion of the small molecules, thus

$$J_{\mathrm{o,PDia}} = Q_{\mathrm{uf,P}} K_{\mathrm{o,PDia}} c_{\mathrm{o,P}}, \tag{2.21}$$

where $Q_{\mathrm{uf,P}}$ is the ultrafiltration rate.

2.3 Fluid volume auxiliary equations

Microvascular filtration

A simple model to describe the microvascular filtration between plasma and interstitial volume was proposed in [29]. We used this approach with the parameters given in that report. For calculating the colloid osmotic pressure we also used a variation (see [30]) to compare these two approaches.

The fluid dynamics model given in [29] uses the Starling equation to calculate the microvascular filtration $Q_{\mathrm{f,PI}}$ where

$$Q_{\mathrm{f,PI}} = K_{\mathrm{f}}(p_{\mathrm{C}} - p_{\mathrm{I}} - \pi_{\mathrm{P}} + \pi_{\mathrm{I}} + p_{\mathrm{off}}), \tag{2.22}$$

and where K_{f} is the capillary filtration coefficient, p_{C} and p_{I} are the pressures in the capillaries and the interstitium, π_{P} and π_{I} are the colloid osmotic pressures in the plasma and the interstitium, respectively, and p_{off} is an offset pressure.

The relationship between the dynamic pressure in the interstitium in regards to the fluid volume of the interstitium and the capillary pressure in regards to the plasma volume were approximated by

$$p_{\mathrm{I}} = aV_{\mathrm{I}} + b/(V_{\mathrm{I}} + c), \tag{2.23}$$

$$p_{\mathrm{C}} = d(V_{\mathrm{P}} + V_{\mathrm{RBC}} + e)^{f}. \tag{2.24}$$

The colloid osmotic pressures were calculated according to [29] by the Landis-Pappenheimer equation [31]:

$$\pi_{\mathrm{P}} = k_1 c_{\mathrm{P}} + k_2 c_{\mathrm{P}}^2 + k_3 c_{\mathrm{P}}^3, \tag{2.25}$$

$$\pi_{\mathrm{I}} = k_1 c_{\mathrm{I}} + k_2 c_{\mathrm{I}}^2 + k_3 c_{\mathrm{I}}^3, \tag{2.26}$$

where $c_{\mathrm{P}} = m_{\mathrm{P}}/V_{\mathrm{P}}$ is the protein concentration in the plasma and $c_{\mathrm{I}} = m_{\mathrm{I}}/V_{\mathrm{I}}$ the protein concentration in the interstitium.

As mentioned above, we also used a second approach to calculate the colloid osmotic pressures by Geranton *et al.* [30]:

$$\pi_{\mathrm{P}} = k_{\mathrm{var}} c_{\mathrm{P}} + c, \tag{2.27}$$

$$\pi_{\mathrm{I}} = k_{\mathrm{var}} c_{\mathrm{I}} + c, \tag{2.28}$$

with the constant c disappearing in the Starling equation (2.22).

3 Results

3.1 Simulations

We exhibit four different cases – healthy persons who undergo orthostatic stress with either shortly increasing or constant lymph flow, and dialysis patients at ultrafiltration with either increasing or decreasing lymph flow during the treatment.

We model these cases, because the dynamics of the lymph flow are unknown under these situations and in fact estimating the lymph flow is one of the goals of this research.

Steady state results match the values found by experiments (see Table 3).

Most parameters were set according to literature. For some other parameters derivations are given in the Appendix p. 19.

Healthy subjects under orthostatic stress

For modeling orthostatic stress, we assume that the capillary pressure is increased to twice its original value. The lymph flow was set to 0.002 L/min and was quickly increased by 100 % in Fig. 1. Lymph flow was constant during the orthostatic test in Fig. 2.

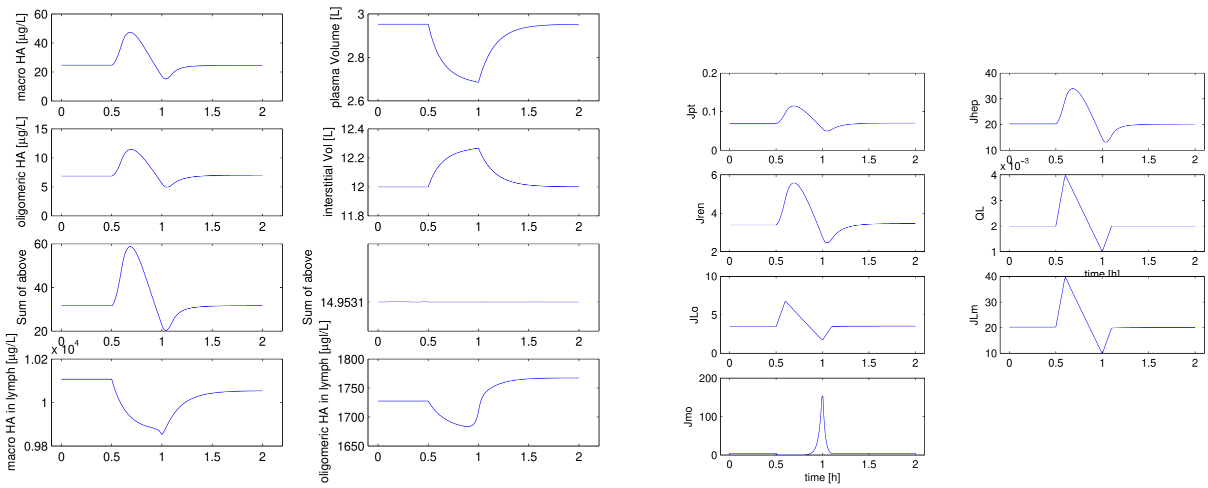

Figure 1: Model output: Healthy person with shortly increasing lymph flow at orthostatic stress

Dialysis patients at ultrafiltration

Ultrafiltration was modeled as a square pulse in a specified interval. The rate of ultrafiltration was assumed to be $Q_{\mathrm{uf,P}} = 0.02$ L/min. The lymph flow Q_{LP} was set to 0.08 L/min for dialysis patients (see [29]), but was increased or decreased during ultrafiltration by 25 % for the Figures 3 and 4, respectively.

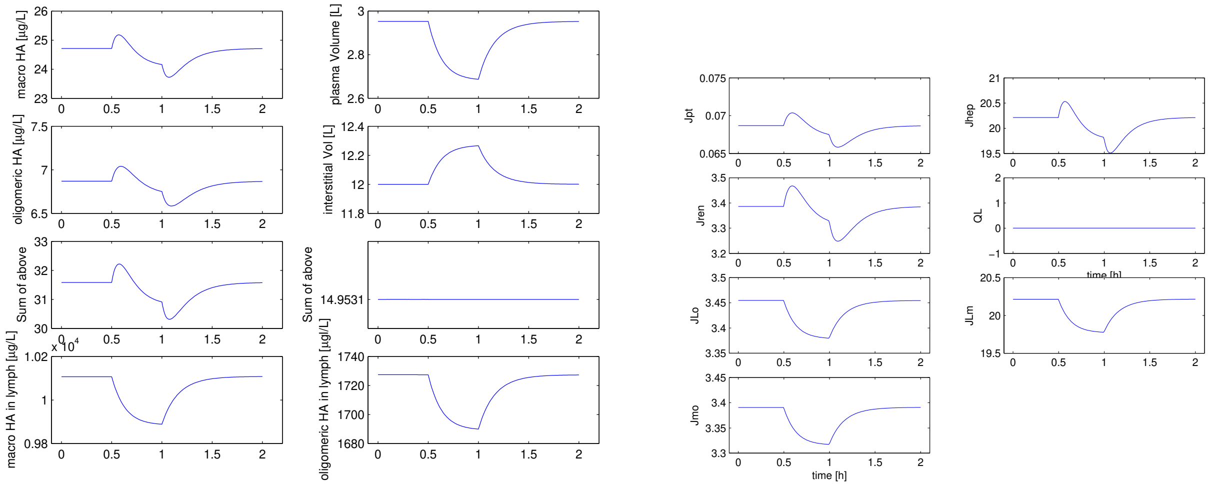

Figure 2: Model output: Healthy person with constant lymph flow at orthostatic stress

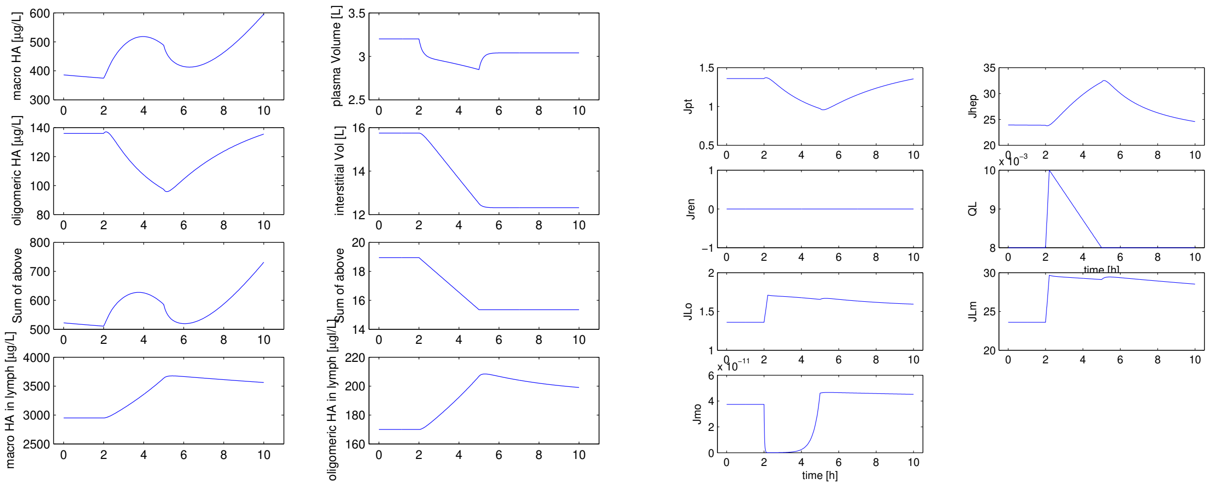

Figure 3: Model output: Dialysis patient with increasing lymph flow at ultrafiltration

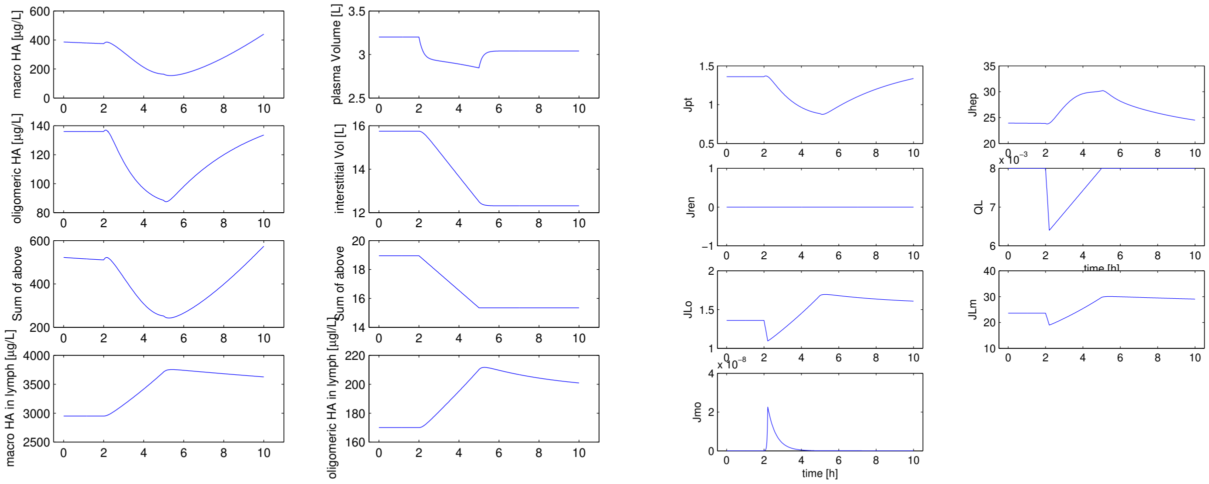

Figure 4: Model output: Dialysis patient with decreasing lymph flow at ultrafiltration

3.2 Sensitivity analysis

Given a system of ODEs

$$\frac{d}{dt}x(t) = f(x(t), t, p), \tag{3.1}$$

where x is a vector of the states of the system, t is the time variable, and p is a vector of system parameters, sensitivity analysis provides the sensitivity $S_{i,j}$ of a state x_i to changes in the parameter p_j. That is,

$$S_{i,j} = \frac{\partial x_i}{\partial p_j}. \tag{3.2}$$

At steady state there exist data sets distinguishing between small and large molecules, but most dynamical data sets available provide only the time course of total concentration of hyaluronan.

As example of sensitivity analysis output we present a case with renal failure including a dialysis treatment from 1.5 to 4.5 hours, during which the lymph flow is decreasing to 0.8 times its original value.

We calculated the sensitivities of the plasma volume and the total hyaluronan concentration in the plasma at ultrafiltration – these sensitivities are plotted in Figures 5 and 6, respectively. The sensitivities may be interpreted as "necessary accuracy" for the parameters. A change in the parameter p_j by the amount of 1 changes the state x_i approximately by $S_{i,j}$.

To compare the sensitivities of a state to several parameters it is more useful to compare relative changes in the parameters by using the normalized sensitivities given by

$$S^n_{i,j} = p_j \frac{\partial x_i}{\partial p_j}. \tag{3.3}$$

This value is an approximation to the state change according to a 100 % change of the parameter. The numbers in the boxes denote mean normalized sensitivity over the plotted interval.

In the upper left edge of Figure 5 there is a plot of the plasma volume over the given time interval. The sensitivity of this state depending on the respective parameter is represented by the other plots. It is obvious that the volume does not depend on the parameters of the hyaluronan auxiliary equations.

If the shape of the curves of two parameters are the same, the volume has a similar dependency on these two parameters – regarding parameter estimation this means that they can not be distinguished using this set of data.

The numbers in the boxes show, that the mass of proteins in the plasma m_{P} determines the plasma volume most. The plasma volume is much less sensitive to the constants f and k_1. The varied osmotic pressure calculation makes the m_{P} much less important.

Figure 6 shows the sensitivities of total hyaluronan concentration in the plasma in respect to the model parameters. The output is most sensitive to Q_{LP}, which we would like to identify with the model, but also very sensitive to the parameters $\bar{v}_{\mathrm{m,Hep}}$, Q_{Hep}, $K_{\mathrm{o,Hep}}$, and $K_{\mathrm{o,PI}}$.

$\bar{v}_{\mathrm{m,Hep}}$, $K_{\mathrm{o,Hep}}$, and $K_{\mathrm{o,PI}}$ are assumed to be constant during ultrafiltration. Consequently we have to have data or at least a good approximation for the dynamics of Q_{Hep} if we want to identify Q_{LP}.

For comparison we also give the sensitivity plots for the orthostase treatments with shortly increasing lymph flow in Figures 7 and 8.

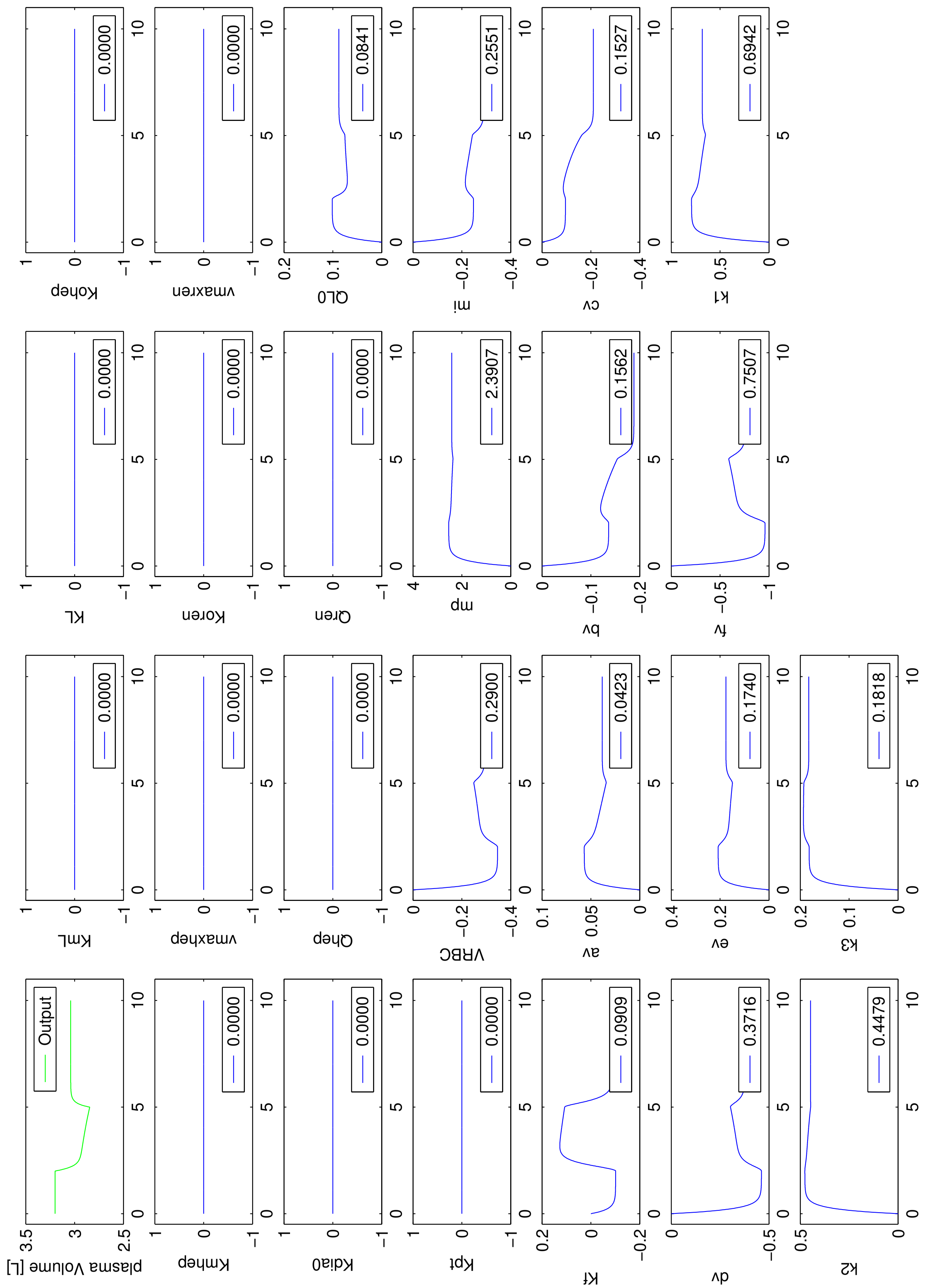

Figure 5: Sensitivity analysis for a dialysis patient with decreasing lymph flow at ultrafiltration: sensitivity of plasma volume is given in respect to changes in model parameters.

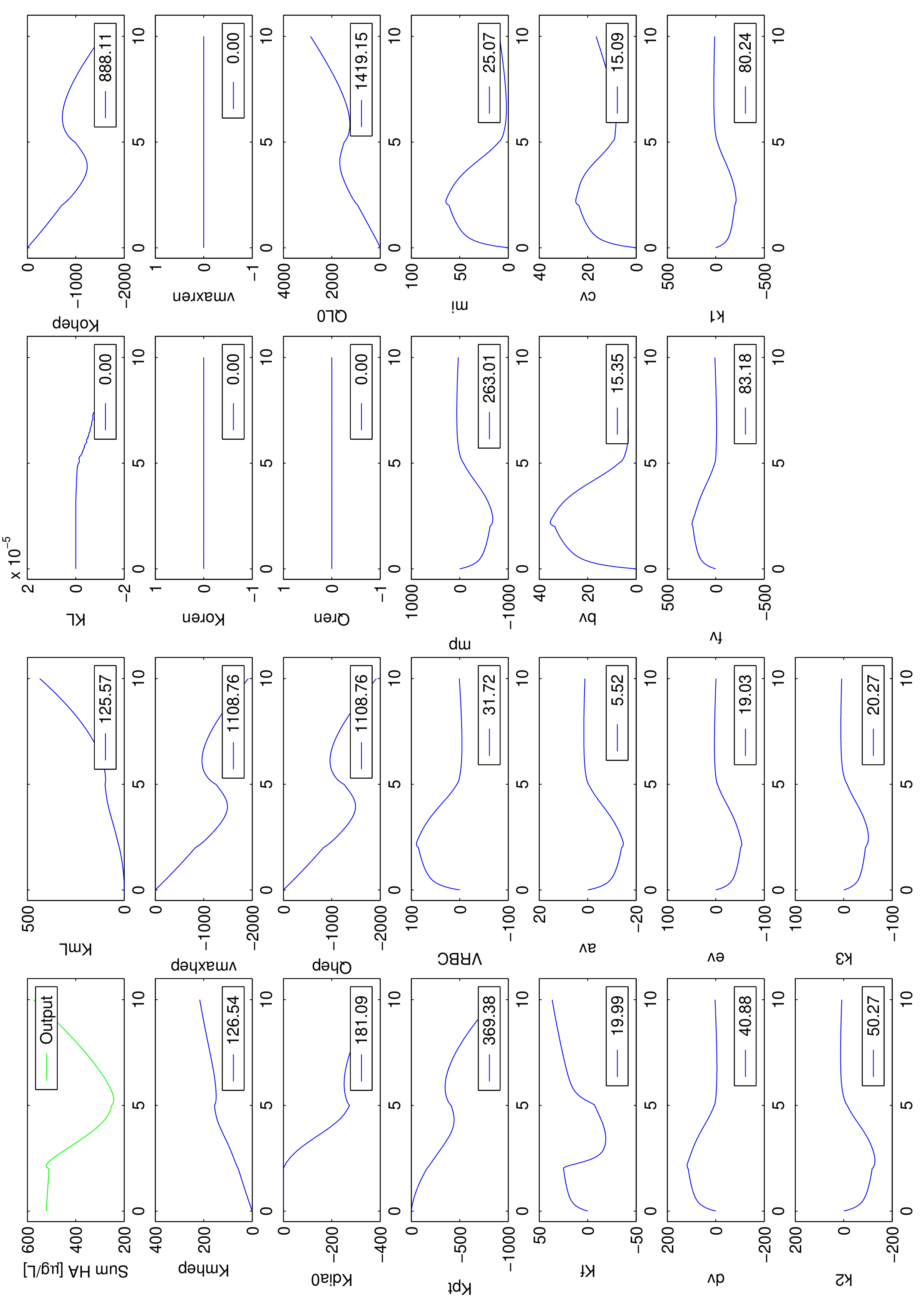

Figure 6: Sensitivity analysis for a dialysis patient with decreasing lymph flow at ultrafiltration: sensitivity of total hyaluronan concentration in the blood is given in respect to changes in model parameters.

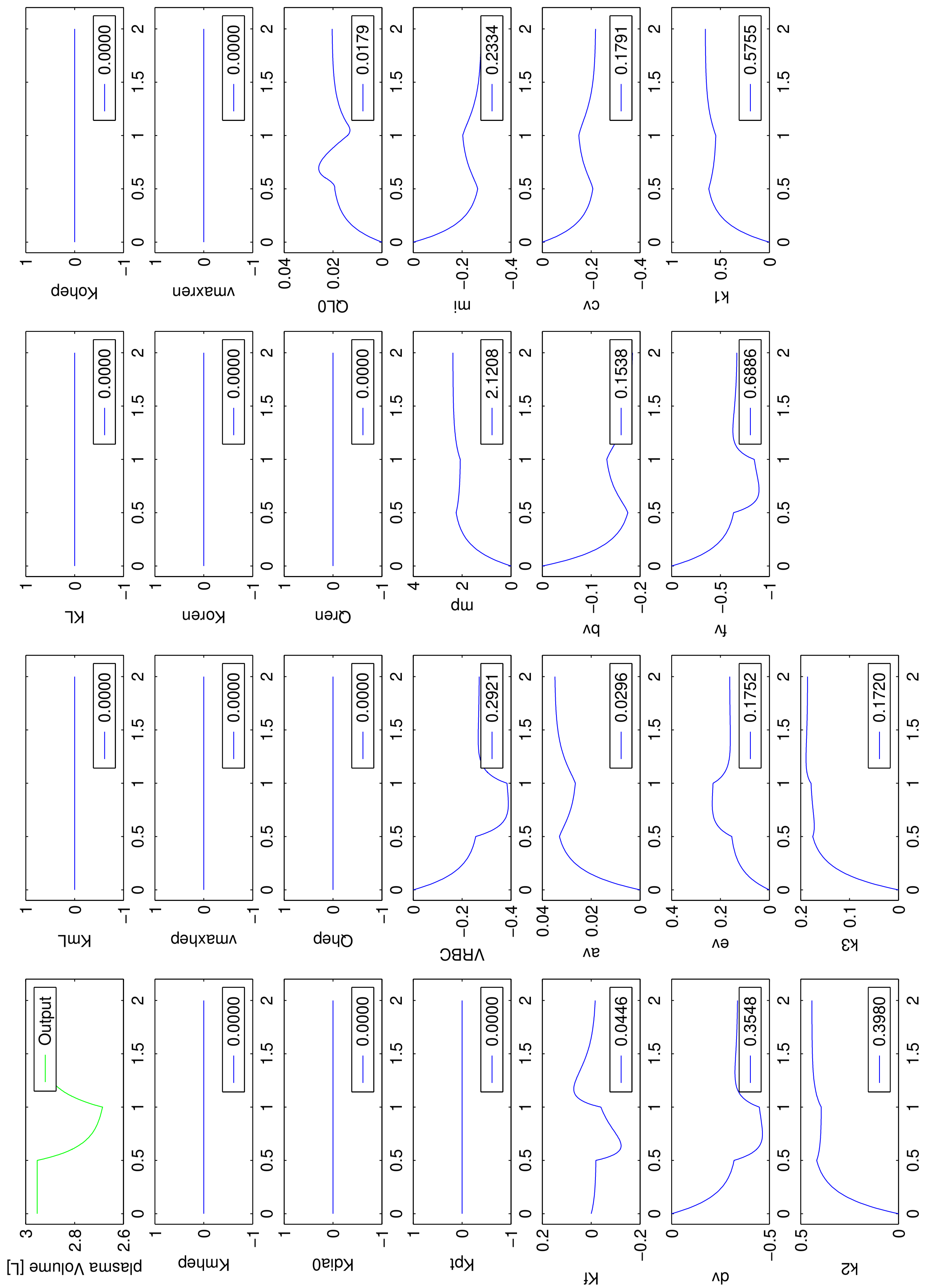

Figure 7: Sensitivity analysis for a healthy human with increasing lymph flow at orthostase: sensitivity of plasma volume is given in respect to changes in model parameters.

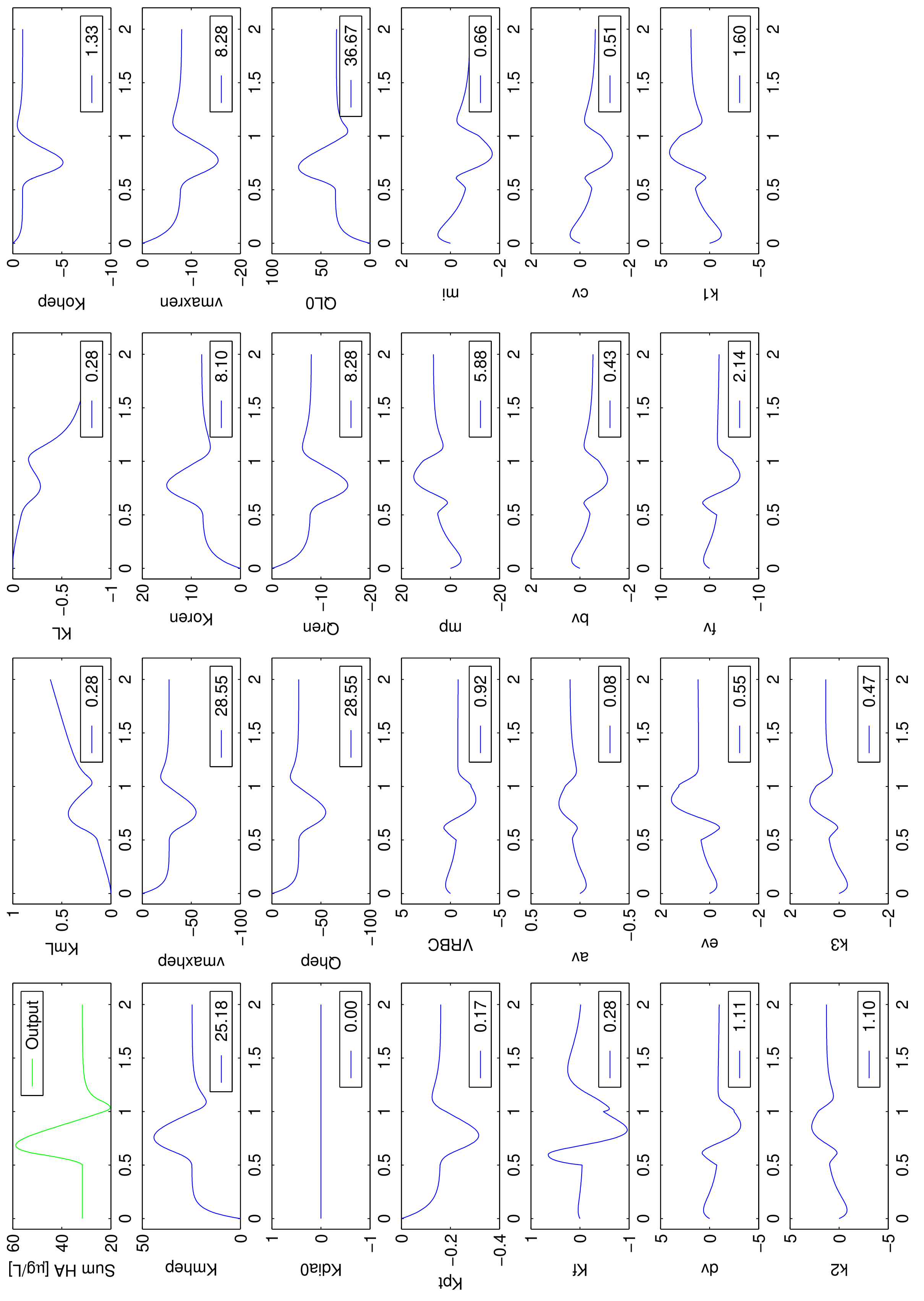

Figure 8: Sensitivity analysis for a healthy human with increasing lymph flow at orthostase: sensitivity of total hyaluronan concentration in the blood is given in respect to changes in model parameters.

3.3 Discussion

The developed model is able to produce reasonable steady states for orthostasis using parameters from literature, but the results for dialysis treatments are not completely representative of the clinical situation.

It seems reasonable that dynamic data from LMWHA and HMWHA would provide better background to fit the parameters and to get a better idea of the quality of the model.

There is at least one issue which has to be further discussed and clarified to improve the model: What is the mechanism behind the decrease of HA concentration in plasma, when the lymph flow is increased?

Up to now our model is able to produce this decrease below the initial steady state before the end of orthostase (see Figures 1 and 2), but if the lymph flow would increase up to five times of its initial value, this undershoot is gone.

The higher the lymph flow is, the higher is the HA plasma concentration, as the HA concentration in the lymph is much higher than that in the plasma. Thus there has to be some counter mechanism which either decreases lymph flow, decreases HA lymph concentration or increases HA excretion from the plasma to get an undershoot at high levels of lymph flow.

Another improvement of the dialysis simulations may be to decouple the volume changes from interstitial and lymph compartments, so that the HA concentration in the lymph wouldn't increase that much. It would be easier to produce the undershoot with this configuration.

A Model equations

The ODEs:

$$\frac{d}{dt}m_{\mathrm{m,P}} = J_{\mathrm{m,LP}} - J_{\mathrm{m,PHep}}, \tag{A.1}$$

$$\frac{d}{dt}m_{\mathrm{o,P}} = J_{\mathrm{o,LP}} - J_{\mathrm{o,PRen}} - J_{\mathrm{o,PI}} - J_{\mathrm{o,PDia}}, \tag{A.2}$$

$$\frac{d}{dt}m_{\mathrm{m,L}} = J_{\mathrm{m,0L}} - J_{\mathrm{m,LP}} - J_{\mathrm{mo,L}}, \tag{A.3}$$

$$\frac{d}{dt}m_{\mathrm{o,L}} = J_{\mathrm{mo,L}} + J_{\mathrm{o,PI}} - J_{\mathrm{o,LP}}, \tag{A.4}$$

$$\frac{d}{dt}V_{\mathrm{P}} = Q_{\mathrm{LP}} - Q_{\mathrm{f,PI}} - Q_{\mathrm{uf,P}}, \tag{A.5}$$

$$\frac{d}{dt}V_{\mathrm{I}} = Q_{\mathrm{f,PI}} - Q_{\mathrm{LP}}. \tag{A.6}$$

The hyaluronan auxiliary equations:

$$J_{\mathrm{m,0L}} = K_{\mathrm{m,0L}}, \tag{A.7}$$

$$J_{\mathrm{mo,L}} = c_{\mathrm{m,L}} e^{-K_{\mathrm{mo,L}} Q_{\mathrm{LP}}}, \tag{A.8}$$

$$J_{\mathrm{m,LP}} = c_{\mathrm{m,L}} Q_{\mathrm{LP}}, \tag{A.9}$$

$$J_{\mathrm{o,LP}} = c_{\mathrm{o,L}} Q_{\mathrm{LP}}, \tag{A.10}$$

$$J_{\mathrm{o,PI}} = K_{\mathrm{o,PI}} c_{\mathrm{o,P}}, \tag{A.11}$$

$$J_{\mathrm{o,PRen}} = Q_{\mathrm{Ren}} \tilde{J}_{\mathrm{ren}} = \frac{Q_{\mathrm{Ren}} \bar{v}_{\mathrm{o,Ren}} c_{\mathrm{o,P}}}{K_{\mathrm{o,Ren}} + c_{\mathrm{o,P}}}, \tag{A.12}$$

$$J_{\mathrm{m,PHep}} = Q_{\mathrm{Hep}} \tilde{J}_{\mathrm{hep}} = \frac{Q_{\mathrm{Hep}} \bar{v}_{\mathrm{m,Hep}} c_{\mathrm{m,P}}}{K_{\mathrm{m,Hep}} + c_{\mathrm{m,P}} \left(1 + \frac{c_{\mathrm{o,P}}}{K_{\mathrm{o,Hep}}}\right)}, \tag{A.13}$$

$$J_{\mathrm{o,PDia}} = Q_{\mathrm{uf,P}} K_{\mathrm{o,PDia}} c_{\mathrm{o,P}}, \tag{A.14}$$

with $c_{\mathrm{m,P}} = m_{\mathrm{m,P}}/V_{\mathrm{P}}$, $c_{\mathrm{o,P}} = m_{\mathrm{o,P}}/V_{\mathrm{P}}$, $c_{\mathrm{m,L}} = m_{\mathrm{m,L}}/V_{\mathrm{I}}$, and $c_{\mathrm{o,L}} = m_{\mathrm{o,L}}/V_{\mathrm{I}}$.

The fluid volume auxiliary equations:

$$Q_{\mathrm{f,PI}} = K_{\mathrm{f}}(p_{\mathrm{C}} - p_{\mathrm{I}} - \pi_{\mathrm{P}} + \pi_{\mathrm{I}} + p_{\mathrm{off}}), \tag{A.15}$$

$$p_{\mathrm{I}} = aV_{\mathrm{I}} + b/(V_{\mathrm{I}} + c), \tag{A.16}$$

$$p_{\mathrm{C}} = d(V_{\mathrm{P}} + V_{\mathrm{RBC}} + e)^f, \tag{A.17}$$

$$\pi_{\mathrm{P}} = k_1 c_{\mathrm{P}} + k_2 c_{\mathrm{P}}^2 + k_3 c_{\mathrm{P}}^3, \tag{A.18}$$

$$\pi_{\mathrm{I}} = k_1 c_{\mathrm{I}} + k_2 c_{\mathrm{I}}^2 + k_3 c_{\mathrm{I}}^3, \tag{A.19}$$

$$\pi_{\mathrm{P}} = k_{\mathrm{var}} c_{\mathrm{P}} + c, \tag{A.20}$$

$$\pi_{\mathrm{I}} = k_{\mathrm{var}} c_{\mathrm{I}} + c. \tag{A.21}$$

B Parameter derivation

As mentioned in the introduction about 25 % of plasma HA is eliminated per minute. Using the measured values from Rössler (see Table 3) and assuming $V_\mathrm{P} = 3$ liters this yields

$$\begin{aligned} J_{\mathrm{o,PRen}} + J_{\mathrm{m,PHep}} &= 0.25(m_{\mathrm{m,P}} + m_{\mathrm{o,P}}) && \text{(B.1)}\\ &\approx 0.25(24.6 \cdot 3.0 + 6.7 \cdot 3.0) && \text{(B.2)}\\ &= 23.475\ \mu\mathrm{g/min}. && \text{(B.3)} \end{aligned}$$

This amount is similar to the endogenous influx of HA as proposed by Laurent *et al.* [32] to be 34 mg/24 h (=23.6 μg/min).

Bentsen *et al.* [25] state that the net hepato-splanchnic extraction ratio of HA is about 33 % and that average net renal extraction ratio of HA in normal kidneys is approximately 20 %.

The net extraction ratio is given by $\frac{\Delta c}{c}$, which gives for the renal component (again assuming a plasma volume of 3 liters):

$$\frac{\Delta c_{\mathrm{o,P}}}{c_{\mathrm{o,P}}} = \frac{J_{\mathrm{o,PRen}}/3}{c_{\mathrm{o,P}}} = 0.2 \tag{B.4}$$

$$\Rightarrow J_{\mathrm{o,PRen}} = 0.6 c_{\mathrm{o,P}} \tag{B.5}$$

$$\Rightarrow Q_{\mathrm{Ren}} \frac{\bar{v}_{\mathrm{o,Ren}} c_{\mathrm{o,P}}}{K_{\mathrm{o,Ren}} + c_{\mathrm{o,P}}} = 0.6 c_{\mathrm{o,P}} \tag{B.6}$$

$$\Rightarrow \bar{v}_{\mathrm{o,Ren}} = \frac{0.6}{Q_{\mathrm{Ren}}}(K_{\mathrm{o,Ren}} + c_{\mathrm{o,P}}) = K_{\mathrm{o,Ren}} + c_{\mathrm{o,P}} \approx 345\ \mu\mathrm{g/L}. \tag{B.7}$$

An analog calculation for the liver yields

$$\bar{v}_{\mathrm{m,Hep}} = \frac{1}{Q_{\mathrm{Hep}}}(K_{\mathrm{m,Hep}} + c_{\mathrm{m,P}}(1 + \frac{c_{\mathrm{o,P}}}{K_{\mathrm{o,Hep}}})) \approx 470\ \mu\mathrm{g/L}. \tag{B.8}$$

On the other hand using equation (B.5) and the hepatitic analog we get a total excretion of

$$J_{\mathrm{o,PRen}} + J_{\mathrm{m,PHep}} = 0.6 c_{\mathrm{o,P}} + 1.0 c_{\mathrm{m,P}} = 28.62\ \mu\mathrm{g/L}, \tag{B.9}$$

which is too much excretion for an inflow of 23.6 μg/min (as derived above), so we decrease these calculated maximal velocities a little.

Symbol	Description	Value	Unit
$K_{\mathrm{m,0L}}$	constant inflow of HMWHA into the lymph	23.6	μg/min
$K_{\mathrm{mo,L}}$	shredding duration	4000	min/L
$K_{\mathrm{o,PI}}$	const. for small HA flow plasma to interst.	0.01	μg/(μg/L)
$K_{\mathrm{o,Hep}}$	inhibitory constant for small HA at liver	12.3	μg/L
$K_{\mathrm{m,Hep}}$	Michaelis constant for large HA at liver	340	μg/L
$\bar{v}_{\mathrm{m,Hep}}$	maximal clearance of large HA by the liver	387	μg/L
$K_{\mathrm{o,Ren}}$	Michaelis constant for small HA at kidney	340	μg/L
$\bar{v}_{\mathrm{o,Ren}}$	maximal clearance of small HA by the kidney	285	μg/L
$K_{\mathrm{o,PDia}}$	clearance of small HA by ultrafiltration	0.60	μg/μg
Q_{Hep}	blood flow to liver	0.8	L/min
Q_{Ren}	blood flow to kidney	0.6	L/min
Q_{LP}	lymph flow (normal/dialysis)	0.002/0.008	L/min
$Q_{\mathrm{uf,P}}$	Ultrafiltration rate	0.02	L/min

Table 1: Parameters of the hyaluronan part of the model

Symbol	Description	Value	Unit
V_{I0}	initial interstitial volume (normal/dialysis)	12/15.75	L
V_{RBC}	volume of red blood cells in blood	2	L
m_{P}	mass of proteins in plasma	210	g
m_{I}	mass of proteins in interstitium	210	g
K_{f}	capillary filtration coefficient	0.0057	L/min mmHg
a	constant for calc. interstitial fluid pressure	0.05	mmHg/L
b	constant for calc. interstitial fluid pressure	-17.5	mmHg L
c	constant for calc. interstitial fluid pressure	-6.5	L
d	constant for calc. capillary pressure	0.8	mmHg/L^f
e	constant for calc. capillary pressure	-1.2	L
f	constant for calc. capillary pressure	1.5	
k_1	constant for calc. COP (V1)	0.21	mmHg/ (g/L)
k_2	constant for calc. COP (V1)	0.0016	mmHg/ (g/L)^2
k_3	constant for calc. COP (V1)	9e-6	mmHg/ (g/L)^3
p_{off}	offset pressure for volume changes (V1)	14.0	mmHg
k_subv	constant for calc. COP (V2)	0.0689	mmHg/ (g/L)
p_{off}	offset pressure for volume changes (V2)	-3.0	mmHg

Table 2: Parameters of the fluid volume part of the model. V1 is calculating the colloid osmotic pressure (COP) according to [29], V2 according to [30]

	absolute (μg/L)	Healthy subjects	ESRD patients Pre dialysis	ESRD patients Post dialysis
measured	Low molecule weight HA	6.7 ± 0.2	135.2 ± 14.4	124.4 ± 13.1
	High molecule weight HA	24.6 ± 1.4	386.0 ± 58.7	237.4 ± 37.7
	Total protein	62.9 ± 0.5	61.2 ± 0.5	66.3 ± 0.7
model	Low molecule weight HA	6.87	136.00	100.80
	High molecule weight HA	24.71	386.00	245.60

Table 3: Measured steady state values are from Rössler (publication in preparation) and states simulated from the model.

Symbol	Description	Steady state values			Unit
		Healthy	Before UF	After UF	Unit
$m_{\mathrm{m,P}}$	mass of macromolecular HA in plasma	72.98	1235.45	746.25	μg
$m_{\mathrm{o,P}}$	mass of oligomeric HA in plasma	20.28	435.29	306.27	μg
$m_{\mathrm{m,L}}$	mass of macromolecular HA in lymph	121283	46463	45628	μg
$m_{\mathrm{o,L}}$	mass of oligomeric HA in lymph	20729	2677	2564	μg
V_{P}	plasma volume	2.95	3.20	3.04	L
V_{I}	interstitial volume	12.00	15.75	12.30	L
$J_{\mathrm{mo,L}}$	degradation of HMWHA to LMWHA in lymph	3.39	3.74E-11	4.70E-11	μg/min
$J_{\mathrm{m,LP}}$	flow of HMWHA from lymph into plasma	20.21	23.60	29.69	μg/min
$J_{\mathrm{o,LP}}$	flow of LMWHA from lymph into plasma	3.45	1.36	1.67	μg/min
$J_{\mathrm{o,PI}}$	diffusion of LMWHA from plasma to tissue through vessel walls	0.069	1.36	1.01	μg/min
$J_{\mathrm{o,PRen}}$	excretion of LMWHA by the kidney	3.39	0	0	μg/min
$J_{\mathrm{m,PHep}}$	excretion of HMWHA by the liver	20.21	23.93	29.26	μg/min
$J_{\mathrm{o,PDia}}$	clearance of oligomeric HA by dialysis filter	0	0	0	μg/min
$Q_{\mathrm{f,PI}}$	microvascular filtration	0.002	0.008	0.008	L
p_{I}	interstitial fluid pressure	-2.58	-1.10	-2.40	mmHg
p_{C}	capillary pressure	5.82	6.40	6.02	mmHg
π_{P}	colloid osmotic pressure in plasma	26.26	23.21	25.13	mmHg
π_{I}	colloid osmotic pressure in interstitium	4.21	3.11	4.10	mmHg

Table 4: Steady states and auxiliary values for orthostase (Fig. 1) and dialysis (Fig. 4) treatments. UF is short for ultrafiltration in dialysis patients (values for -20 % lymph flow during UF).

References

[1] K Meyer and J W Palmer. The polysaccharide of the vitreous humor. *J Biol Chem*, 109:386–394, 1934.

[2] J H Fessler and L I Fessler. Electron microscopic visualization of the polysaccharide hyaluronic acid. *Proc Natl Acad Sci USA*, 56:141–147, 1966.

[3] P Prehm. Hyaluronate is synthesized at plasma membranes. *Biochem J*, 220:597–600, 1984.

[4] H J Granger. Physicochemical properties of intestinal and liver edema. In A R Hargens, editor, *Tissue Fluid Pressure and Composition*, pages 43–63. Williams & Wilkins, Baltimore, 1981.

[5] W D Comper and T C Laurent. Physiological function of connective tissue polysaccharides. *Physiol Rev*, 58:255–315, 1978.

[6] H A Koomans, A B Geers, and E J Dorhout Mees. Plasma volume recovery after ultrafiltration in patients with chronic renal failure. *Kidney Int*, 26:848–854, 1984.

[7] A Tengblad, U B G Laurent, K Lilja, R N P Cahill, A Engström-Laurent, J R R Fraser, H E Hansson, and T C Laurent. Concentration and molecular mass of hyaluronate in lymph and blood. *Biochem J*, 236:521–525, 1986.

[8] R J Fraser, W G Kimpton, T C Laurent, R N Cahill, and N Vakakis. Uptake and degradation of hyaluronan in lymphatic tissue. *Biochem J*, 256:153–158, 1988.

[9] T J Brown, W G Kimpton, and J R Fraser. Biosynthesis of glycosaminoglycans and proteoglycans by the lymph node. *Glycoconj J*, 17:795–805, 2000.

[10] A Rössler and H Hinghofer-Szalkay. Hyaluronan fragments: an information-carrying system? *Horm Metab Res*, 35:67–68, 2003.

[11] B Smedsrod, H Pertoft, S Eriksson, J R E Fraser, and T C Laurent. Studies in vitro on the uptake and degradation of sodium hyaluronate in rat liver endothelial cells. *Biochem J*, 233:617–626, 1984.

[12] J Lesley, V C Hascall, M Tammi, and R Hyman. Hyaluronan binding by cell surface CD44. *J Biol Chem*, 275(35):26967–26975, 2000.

[13] J R E Fraser, L E Appelgren, and T C Laurent. Tissue uptake of circulating hyaluronic acid. A whole-body autoradiographic study. *Cell Tiss Res*, 233:285–293, 1983.

[14] A Engström-Laurent, U B G Laurent, K Lilja, and T C Laurent. Concentration of sodium hyaluronate in serum. *Scand J Lab Invest*, 45:497–504, 1985.

[15] A Rössler, Z László, E Kvas, and H G Hinghofer-Szalkay. Plasma hyaluronan concentration: no circadian rhythm but large effect of food intake in humans. *Eur J Appl Physiol*, 78:573–577, 1998.

[16] K Aukland and G Nicolaysen. Interstitial fluid volume: local regulatory mechanisms. *Physiol Rev*, 61(3):556–643, 1981.

[17] G Szabo and Z Magyar. Pressure measurements in various parts of the lymphatic system. *Acta Medica*, 23:237–241, 1967.

[18] M Aas, A Skretting, A Engeset, R Westgaard, and G Nicolaysen. Lymphatic drainage from subcutaneous tissue in the foot and leg in the sitting human. *Acta Physiol Scand*, 125:505–511, 1985.

[19] R Entrup, D Paiewonsky, M Hughes, J Jue, D Bittar, and R Wégria. Effect of posture on formation and evacuation of lymph. *Am J Physiol*, 210:943–949, 1966.

[20] E M Renkin, W L Joyner, C H Sloop, and P D Watson. Influence of venous pressure on plasma-lymph transport in the dog's paw: convective and dissipative mechanisms. *Microvasc Res*, 14:191–204, 1977.

[21] M A Katz. Interstitial space – the forgotten organ. *Med Hypoth*, 6:885–898, 1980.

[22] K Aukland. Why don't our feet swell in the upright position? *NIPS*, 9:214–219, 1994.

[23] M Ziegler. Postural hypotension. *Ann Rev Med*, 31:239–245, 1980.

[24] R Beeuwkes, I Ichikawa, and B M Brenner. The renal circulation. In B M Brenner and F C Rector, editors, *The kidney*, volume 1, pages 249–288. W.B. Saiunders Company, Philadelphia, London, Toronto, 1981.

[25] K D Bentsen, J H Henriksen, and T C Laurent. Circulating hyaluronate: concentration in different vascular beds in man. *Clin Sci*, 71:161–165, 1986.

[26] W L Olszewski. Physiology and microsurgery of lymphatic vessels in man. *Lymphology*, 14:44–60, 1981.

[27] G Szabo, Z Magyar, and M Papp. Correlation between capillary filtration and lymph flow in venous congestion. *Acta Med Acad Sci Hung*, 19:185–191, 1963.

[28] J Keener and J Sneyd. Interdisciplinary applied mathematics. In J E Marsden, L Sirovich, and S Wiggins, editors, *Mathematical physiology*, volume 8. Springer-Verlag, New York, 2001.

[29] R Pilgram, W Ring, and D Schneditz. Optimized identification of fluid volume and hematocrit during ultrafiltration. Technical Report 220, SRC F-003, University of Graz, Austria, 2001.

[30] F Geranton, F Chantrel, M Bouiller, S Muller, I Kolb, B Moulin, and T Hannedouche. Prediction of colloid osmotic pressure in renal patients. *Clin Nephrol*, 53(4):67–68, 2000.

[31] E M Landis and J R Pappenheimer. Exchange of substances through the capillary walls. In W F Hamilton and P Dow, editors, *Handbook of Physiology*, pages 961–1024. American Physiological Society, Washington, DC, 1963.

[32] T C Laurent and J R E Fraser. Hyaluronan. *Faseb J*, 6:2397–2404, 1992.